IEEE Access
Multidisciplinary ⋮ Rapid Review ⋮ Open Access Journal

Received 11 July 2024, accepted 10 August 2024, date of publication 14 August 2024, date of current version 23 August 2024.

*Digital Object Identifier 10.1109/ACCESS.2024.3443695*

RESEARCH ARTICLE

# Enhancement of Photovoltaic Performance With Coolant Calcium Chloride: Experimental and Predictive Modeling

**ASRI[1,2], (Student Member, IEEE), YUWALDI AWAY[3], (Member, IEEE), NASARUDDIN[3], (Member, IEEE), IRA DEVI SARA[3], (Member, IEEE), AND ANDRI NOVANDRI[3], (Student Member, IEEE)**

[1]Doctoral Program of Engineering, Universitas Syiah Kuala, Banda Aceh 23111, Indonesia
[2]Department of Electrical Engineering, Universitas Malikussaleh, Lhokseumawe 24355, Indonesia
[3]Department of Electrical and Computer Engineering, Universitas Syiah Kuala, Banda Aceh 23111, Indonesia

Corresponding author: Yuwaldi Away (yuwaldi@usk.ac.id)

**ABSTRACT** This paper proposes a new method for predicting the energy generated by Photovoltaic (PV) panels with coolant Calcium Chloride ($CaCl_2$). The study seeks to address heat-related issues that can affect the performance of PV panels by reducing their operational temperature. High operational temperatures can decreased electricity production, potentially cause permanent damage to solar cells, and shorten the panel's lifespan. Calcium Chloride compound possesses hygroscopic properties, meaning it can absorb water from the surrounding air, thus serving as a cooling material. Calcium Chloride compound is applied as crystalline granules placed in a container beneath the PV panel. This research seeks to evaluate the effect of Calcium Chloride usage on reducing the operational temperature of PV panels and its influence on increasing PV efficiency. Subsequently, using the temperature data of the PV panel, modeling is performed to predict the PV output power using three predictive models: Multiple Linear Regression (MLR), Temperature Coefficient of Power (TC-P), and Artificial Neural Network (ANN). These three models are then compared to test their effectiveness. The research results indicate that using Calcium Chloride as a coolant is highly effective in improving the performance and efficiency of PV panels. Additionally, the ANN model accurately predicts power output based on temperature condition variations, with a Coefficient of Determination ($R^2 = 0.98$).

**INDEX TERMS** Photovoltaic, calcium chloride, cooling of PV panels, ANN, MLR, TC-P.

## I. INTRODUCTION

Photovoltaic (PV) systems face significant challenges related to heat issues in renewable energy electricity generation. The performance of PV is greatly influenced by its operational temperature [1], [2], [3]. Elevated temperatures can reduce electricity production, particularly when exposed to intense direct sunlight. [4], [5], [6], [7], [8]. PV temperature affects the generated electrical power due to the photovoltaic effect occurring within the semiconductor material [9], [10], [11], [12]. The semiconductor material absorbs Photon energy from sunlight, creating electron-hole pairs [13], [14], [15]. Elevated temperatures increase the thermal energy of electrons, thereby reducing the energy needed to free them from atomic bonds [16], [17], [18]. Consequently, the efficiency of converting photon energy into electrons decreases, resulting in reduced electrical energy output [19], [20], [21], [22]. Moreover, excessive temperatures can shorten the lifespan of PV systems, even causing permanent damage [23], [24], [25]. Research in [26] shows that temperature is a crucial factor affecting PV performance. The results reveal a decrease in PV maximum power with increasing operational temperature. This decrease ranges from 0.14% to 0.47% for every 1°C increase in temperature.

Many studies have been conducted on PV cooling systems to address this issue. One previous study proposed heatsinks as described in the paper [27]. The heatsink configuration consisted of three heatsinks, each with eight fins

The associate editor coordinating the review of this manuscript and approving it for publication was Youngjin Kim.

made of aluminum, aiming to enhance heat dissipation [28]. Adding these heatsinks successfully reduced the average temperature of the PV panel from 45.8°C to 42.2°C (7.9%). Based on these results, optimization is needed to further enhance the temperature reduction in PV. Therefore, developing a cooling system using Calcium Chloride ($CaCl_2$) was pursued. Calcium Chloride possesses excellent cooling properties and can be applied as a cooling material for PV. Additionally, Calcium Chloride is known as a hygroscopic compound, capable of absorbing moisture from the air, making it highly water-absorbent [29]. The melting point of Calcium Chloride is around 772°C, while its boiling point is approximately 1600°C [30]. With these properties, Calcium Chloride becomes a suitable chemical for cooling material. The cooling process occurs due to the endothermic nature of the Calcium Chloride solution when mixed with water [31]. The compound requires heat energy during this mixing process to break the bonds between calcium ions (Ca2+), chloride ions (Cl-), and water. As a result, the compound absorbs heat energy from its surrounding environment, causing the temperature to decrease and creating a cooling effect [32]. One of the main advantages of using Calcium Chloride as a coolant is its ability to reach lower temperatures than pure water. In some cases, Calcium Chloride material can achieve much lower temperatures than regular salt solutions, making it highly effective in lowering temperatures in various industrial applications [33]. Several studies have investigated Calcium Chloride as a cooling and heat-absorbing agent, as reviewed in the paper [34]. This paper discusses the heat transfer characteristics of Calcium Chloride solutions as gas coolants and evaporators. The results indicate that the solution can reduce heat by up to 15%, thus optimizing thermal effectiveness. Furthermore, the paper [35] discusses using Calcium Chloride as zeolite 13X/$CaCl_2$ composite adsorbents, showing significant potential in enhancing the performance of Adsorption Cooling Systems (ACS). ACS is a system that utilizes the principle of adsorption, where gas molecules are absorbed or trapped from a specific medium, leading to temperature reduction [36]. The research results show that the Specific Cooling Power (SCP), which measures a material's ability to absorb heat, increased by up to 34% compared to pure zeolite 13X. On the other hand, several different types of cooling materials have been studied to reduce the operational temperature of PV. Literature related to PV cooling methods is presented in Table 1. Based on this literature review, it can be concluded that reducing the operational temperature of PV can enhance efficiency and generate electrical power.

Modeling the output power of PV with Calcium Chloride cooling is part of developing this solution by understanding the relationship between the influence of Calcium Chloride on operational temperature and PV output power [37], [38], [39]. This study aims to explore the utilization of Calcium Chloride as a cooling material in PV systems and to simulate its effect on output power. This model shows how the coolant Calcium Chloride system affects electrical power production in PV [40], [41]. This modeling can accurately predict the use of coolant Calcium Chloride systems in influencing the performance and efficiency of PV under various operational and environmental conditions [42], [43], [44], [45], [46]. Several PV power modeling methods are discussed in other literature, such as in papers [47] and [48]. These papers discuss PV power output modeling using Multiple Linear Regression (MLR), a statistical method used to analyze the relationship between one output variable and several input variables, assuming a linear relationship. The results of these papers mention that the MLR model is relatively simple and easy to interpret, thus capable of explaining the linear relationship between the operational temperature variable and the power variable in PV. Furthermore, in the paper [49], modeling is done using the Temperature-Coefficient of Power (TC-P). The TC-P model explains the relationship between output power and PV operational temperature, depicting the power output changes for each specific temperature increase. The paper states that measurement results show a significant relationship between the operational temperature variable and power output, thus allowing the prediction of PV power at specific temperatures. Additionally, in papers [50], [51], [52], [53], modeling methods using Artificial Neural Networks (ANN) are discussed. ANN is a computational model capable of understanding complex data with high accuracy and is thus able to handle various prediction problems. These papers reveal that using ANN can provide accurate results in predicting PV power output.

This study proposes a method of cooling PV using Calcium Chloride to improve efficiency and overall performance in PV. The Calcium Chloride compound used is made of solid material in crystalline granules. This material is placed in a container which is then covered by the PV panel. The heat the PV receives is then directed to the material to be absorbed, thus reducing its operational temperature. To further understand the impact of cooling using Calcium Chloride on PV power output, temperature modeling is conducted using MLR, TC-P, and ANN methods. This modeling can account for the relationship between operational temperature and PV power output, thus enabling the prediction of electrical power generated under various temperature conditions. The performance comparison of these three models is then analyzed to determine the performance of each model. The results of this analysis can aid in selecting the most accurate model for predicting PV power output. Thus, cooling methods using Calcium Chloride can be optimized by modeling PV power. This allows users to make more effective plans for installing solar power plants to assess the available solar energy potential. The main focus of this paper is as follows:

- We propose a method of cooling PV temperature using Calcium Chloride compound as a cooling material.
- We propose modeling methods using MLR, TC-P, and ANN to model the temperature of PV using Calcium Chloride coolant.
- We compare the performance of these three models in predicting PV power output.

**TABLE 1.** Literature review of cooling method for photovoltaic.

| Paper | Year | PV Type | Cooling Method | Measurement Time | Measurement Location | Efficiency Improvement |
|---|---|---|---|---|---|---|
| Ravishankar Sathyamurthy et al. [54] | 2021 | Monocrystalline | CNT/$Al_2O_3$ Hybrid | May 2019 | - | 2.4% |
| Zainal Arifin et al. [55] | 2020 | Polycrystalline | Aluminum Heat Sinks | - | - | 2.6% |
| M.R. Salem et al. [56] | 2019 | Polycrystalline | $Al_2O_3$/PCM Mixture | - | Egypt | 10.9% |
| Munzer.S.Y. Ebaid et al. [57] | 2018 | Monocrystalline | $TiO_2$ | - | Jordan | 0.82% |
| Pratik Mundle et al. [58] | 2018 | Polycrystalline | Aluminum Back Plate | - | India | - |
| Hashim A. Hussein et al. [59] | 2017 | Monocrystalline | Zn/$H_2O$ Mixture | - | Iraq | 7.8% |
| A.R. Amelia et al. [60] | 2016 | Monocrystalline | DC Fan | April 2015 | Malaysia | - |
| K.A. Moharram et al. [61] | 2013 | Monocrystalline | Water | June 2012 | Egypt | 12.5% |

**TABLE 2.** Summary of abbreviations.

| Abbreviation | Meaning |
|---|---|
| ACS | Adsorption Cooling Systems |
| ANN | Artificial Neural Network |
| $CaCl_2$ | Calcium Chloride |
| LCA | Life Cycle Assessment |
| MAE | Mean Absolute Error |
| MLR | Multiple Linear Regression |
| MSE | Mean Squared Error |
| PV | Photovoltaic |
| RMSE | Root Mean Squared Error |
| SCP | Specific Cooling Power |
| STC | Standard Test Conditions |
| TC-P | Temperature Coefficient of Power |

For convenience, the abbreviations used in this paper are summarized in Table 2.

## II. EXPERIMENTAL METHOD

The experiment measured the performance level of using Calcium Chloride as a coolant on PV panels. The Calcium Chloride compound used is in the form of solid crystal particles placed in a square container with a PV panel mounted on top, as shown in Figure 1. Technically, the cooling material is placed at the bottom, adjacent to the PV panel. The specifications of the PV used in this test are listed in Table 3.

Meanwhile, the data in Table 4 depicts the thermal conditions during the testing process, including air temperature, humidity, and duration of sunlight exposure throughout the day. The testing was conducted over three consecutive days in Lhokseumawe, Indonesia. Furthermore, using the data from PV measurements with coolant Calcium Chloride, modeling was performed using three different predictive models: MLR, TC-P, and ANN. This modeling aims to predict PV power output based on varying thermal conditions and PV operational temperatures. These three models were then analyzed to determine the level of accuracy in predicting PV power output.

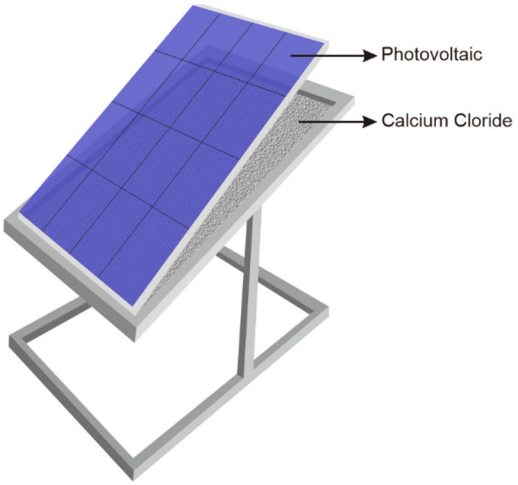


**FIGURE 1.** Placement of Calcium Chloride compound on PV.

**TABLE 3.** Photovoltaic module specification.

| Features | Value |
|---|---|
| Type | Polycrystalline |
| Maximum power ($P_{max}$) | 100Wp |
| Voltage at $P_{max}$ ($V_{mp}$) | 18V |
| Current at $P_{max}$ ($I_{mp}$) | 5.56A |
| Open-circuit voltage ($V_{oc}$) | 21.6V |
| Short-circuit current ($I_{sc}$) | 5.99A |
| Normal operating cell temp (NOCT) | 47 ± 2ºC |
| Operating temperature | 40ºC - 85ºC |

## III. PROPOSED MODELS

### A. MLR MODEL

The MLR model is used to model the linear relationship between input variables and output variables, aiming to understand and predict the influence of input variables on output variables [62]. In this modeling, there are four input variables: ‘‘TempTop’’, which is the temperature data of the top side of the PV panel, while ‘‘TempBot’’ is the bottom side, ‘‘Irradiance’’ is the sunlight irradiance data, and

**TABLE 4.** Thermal conditions during the experiment.

| | Air Temperature (°C) | | | Humidity (%) | Sunshine Duration (hour) |
|---|---|---|---|---|---|
| | Min | Max | Average | | |
| **Day 1** 4th April 2023 | 21.8 | 32.6 | 26.9 | 78 | 3.5 |
| **Day 2** 5th April 2023 | 21.8 | 32.7 | 26.7 | 70 | 7 |
| **Day 3** 6th April 2023 | 20.4 | 33.4 | 26.6 | 72 | 11 |

"Humidity" is the air humidity data. Meanwhile, the output variable is the predicted value, "Power", which is the PV power output. The proposed equation for the MLR model in predicting PV power is as follows,

$$P_{MLR} = \beta_0 + \beta_1.x_1 + \beta_2.x_2 + \beta_3.x_3 + \beta_4.x_4 \quad (1)$$

where, $P_{MLR}$ is the value of the "Power" variable. The variables $\beta_1$, $\beta_2$, $\beta_3$, and $\beta_4$ respectively represent the regression coefficients of "TempTop", "TempBot", "Irradiance", and "Humidity". Meanwhile, the variables $x_1$, $x_2$, $x_3$, and $x_4$ respectively represent the values of "TempTop", "TempBot", "Irradiance", and "Humidity". The variable $\beta_0$ is the intercept coefficient, which can be calculated using the following equation,

$$\beta_0 = \overline{P} - \beta_1.\overline{x_1} - \beta_2.\overline{x_2} - \beta_3.\overline{x_3} - \beta_4.\overline{x_4} \quad (2)$$

where, $\overline{P}$ is the mean value of the "Power" data, while $\overline{x_1}$, $\overline{x_2}$, $\overline{x_3}$, and $\overline{x_4}$ respectively represent the mean values of "TempTop", "TempBot", "Irradiance", and "Humidity" data. Meanwhile, to calculate the regression coefficient values of each variable $\beta_1$, $\beta_2$, $\beta_3$, and $\beta_4$, the following equation is used,

$$\beta_j = \frac{\sum_{i=1}^{n}(x_{ij} - \overline{x_j})(P_i - \overline{P})}{\sum_{i=1}^{n}(x_{ij} - \overline{x_j})^2}; \quad 1 \geq j \geq 4 \quad (3)$$

where, $\beta_j$ represents the regression coefficient of input $j$, $x_{ij}$ is the input $j$ value in data $i$, $\overline{x_j}$ is the mean value of input $j$, $P_i$ is the "Power" value in data $i$, and $\overline{y}$ is the mean value of "Power". Based on the calculation results, the MLR model to predict PV output power is obtained as follows,

$$P_{MLR} = -52.7 + 1.5x_1 + 0.17x_2 + 0.03x_3 + 0.37x_4 \quad (4)$$

Next, MLR analysis was carried out to determine the model's performance. The Standard Error indicates how accurate the coefficient estimates are, while the $t$-statistic and $p$-value assist in analyzing the statistical significance of these coefficients.

Table 5 shows that the variable "Irradiance" has a statistically significant coefficient with a low $p$-value of 0.001. This result indicates a strong influence on the "Power" variable. However, other variables, such as "TempTop", have slightly higher $p$-values, namely 0.065. This value suggests a weaker influence. In contrast, the variable "Humidity" shows no significant relationship with the "Power" variable, as evidenced by the $p$-values of 0.23.

**TABLE 5.** The MLR analysis.

| Variable | Coefficient | Standard Error | $t$-statistic | $p$-value |
|---|---|---|---|---|
| Constant | -52.7 | 36.01 | -1.46 | 0.151 |
| TempTop | 1.5 | 0.79 | 1.9 | 0.065 |
| TempBot | 0.17 | 0.85 | 0.2 | 0.841 |
| Irradiance | 0.03 | 0.01 | 3.64 | 0.001 |
| Humidity | 0.37 | 0.3 | 1.22 | 0.23 |

### B. TC-P MODEL

The TC-P model is used to model the relationship between the output variable, which is the PV power, and the input variable, which is the operational temperature of the PV. The TC-P model estimates PV output power based on specific PV temperatures [63], [64]. The equation for TC-P can be expressed as follows,

$$P_{TCP} = P_{STC}\left(1 + \beta\left(T_{pv} - T_{STC}\right)\right) \quad (5)$$

where, $P_{out}$ is the PV output power at a specific temperature, $P_{STC}$ is the solar panel output power at Standard Test Conditions (STC), which is when irradiance has a value of 1000 W/m$^2$, $T_{pv}$ is the PV temperature under operational conditions, $T_{STC}$ is the PV temperature under STC conditions, and $\beta$ is the power temperature coefficient, which is the percentage change in PV output power for each specific temperature increase [65]. The value of $\beta$ can be calculated using the gradient of the regression line between temperature data and PV output power, which can be computed using the following equation,

$$\beta = \frac{\sum_{i=1}^{n}(x_i - \overline{x})(y_i - \overline{y})}{\sum_{i=1}^{n}(x_i - \overline{x})^2} \quad (6)$$

where, $x_i$ and $y_i$ are the values of each variable in data $i$, $\overline{x}$ and $\overline{y}$ are the mean values of variables $x$ and $y$, and $n$ is the total data.

Based on the calculations using measurement data of 45 instances, the value of $\beta$ is 3.1% per °C or 0.031 per °C. Furthermore, measurements of PV under an irradiance condition of 1000 W/m$^2$, resulted in an output power of 100W with an operational temperature of 50.4°C. Based on these measurement results, the TC-P model is expressed as follows,

$$P_{TCP} = 100\left(1 + 0.031\left(T_{pv} - 50.4\right)\right) \quad (7)$$

### C. ANN MODEL

The ANN model is a computational model inspired by the structure and function of biological neural networks in humans. This model consists of simple processing units called neurons or nodes, interconnected in a network structure comprising multiple layers. This study uses the ANN model

**TABLE 6.** The ANN structure.

| Parameter | Value | Description |
|---|---|---|
| Number of layers | 4 | Number of layers in the ANN architecture |
| Number of input nodes | 4 | Number of nodes in the input layer |
| Number of hidden nodes 1 | 120 | Number of nodes in the hidden layer 1 |
| Number of hidden nodes 2 | 72 | Number of nodes in the hidden layer 2 |
| Number of output nodes | 1 | Number of nodes in the output layer |
| Number of iterations | 5000 | Number of iterations in the training process |
| Learning rate | 0.3 | ANN learning rate parameter |
| Momentum factor | 0.9 | The parameters that affect weight changes |
| Error | 1.67 | Maximum error value achieved after the learning process |
| The activation function of hidden layer 1 | Sigmoid function | The type of activation function used in the hidden layer 1 |
| The activation function of hidden layer 2 | Sigmoid function | The type of activation function used in the hidden layer 2 |
| The activation function of output layer | Sigmoid function | The type of activation function used in the output layer |
| Training method | Back-Propagation | The training method used for the learning process |

to predict PV output power based on variations in temperature and environmental conditions. This proposed ANN model uses four input variables: ''TempTop'', ''TempBot'', ''Irradiance'', and ''Humidity'', with the output variable being ''Power''. Both variables are then trained to understand the patterns of relationships between variables [66]. The proposed ANN network structure can be seen in Table 6.

A learning process consisting of two stages is required to obtain the ANN model: Feed-forward and Back-propagation [67]. Feed-forward is the process where input data is passed through the network from the input layer through the hidden layers to the output layer. In this stage, each node in the layer forwards its input signal by applying an activation function to the nodes in the next layer. This is done so that the ANN can understand the patterns and structure of the given input data. The initial stage of Feed-forward is to calculate the values of the nodes in the hidden layer. In this case, there are two hidden layers. To calculate the values of the nodes in the first hidden layer, the following equation is used,

$$H_x^{(1)} = f\left(\sum_{j=1}^{120}\sum_{i=1}^{4} I_i.H_{wij}^{(1)} + H_{bj}^{(1)}\right) \tag{8}$$

where, $H_x^{(1)}$ is the value of the $x$ node in the first hidden layer, $f$ is the applied activation function, $I_i$ is the value of the $i$ node in the input layer, $H_{wij}^{(1)}$ is the weight value from the $i$ node in the input layer to the $j$ node in the first hidden layer, and $H_{bj}^{(1)}$ is the bias value of the $j$ node in the first hidden layer. The activation function used in both hidden layers employs the sigmoid function, expressed as follows,

$$f(x) = \frac{1}{\left(1 + e^{-x}\right)} \tag{9}$$

where, $e$ is the Euler's number, which is the base of the natural logarithm. Furthermore, calculations are performed to compute the nodes in the hidden layer using the following equation,

$$H_x^{(2)} = f\left(\sum_{j=1}^{72}\sum_{i=1}^{120} H_i^{(1)}.H_{wij}^{(2)} + H_{bj}^{(2)}\right) \tag{10}$$

where, $H_x^{(2)}$ is the value of the $x$ node in the second hidden layer, $H_i^{(1)}$ is the value of the $i$ node in the first hidden layer, $H_{wij}^{(2)}$ is the weight value from the $i$ node in the first hidden layer to the $j$ node in the second hidden layer, and $H_{bj}^{(2)}$ is the bias value of the $j$ node in the second hidden layer. The final step in this Feed-forward process is to calculate the value of the nodes in the output layer. The calculation of the node values in the output layer uses the following equation,

$$O_x = f\left(\sum_{i=1}^{72} H_i^{(2)}.O_{wi} + O_b\right) \tag{11}$$

where, $O_x$ is the output value at the $x$ node, $H_i^{(2)}$ is the value of the $i$ node in the second hidden layer, $O_{wi}$ is the weight value from the $i$ node in the second hidden layer to the node in the output layer, and $O_b$ is the bias value at the output layer.

After the Feed-forward process is completed, the values in the output layer are obtained. These values are then compared with the target data to determine the error. The magnitude of the error indicates how far the predictions deviate from the actual values. To calculate the error, the following equation is used,

$$error = \sum_{i=1}^{n} \frac{1}{2}(T_i - O)^2 \tag{12}$$

where $T_i$ is the target data in the $i$ dataset, while $O$ is the output data.

The following process is Back-propagation, where the prediction results are used to adjust the network model parameters by updating weights and biases, aiming to minimize the error between the model predictions and actual values. To update the bias values in the output layer, the following equation is used,

$$O_b = (T_i - O)(1 - O)O \tag{13}$$

where, $O_b$ is the bias value in the output layer, $T_i$ is the target data in the $i$ dataset, and $O$ is the node's value in the output layer. The following process updates the weight values from the second hidden layer to the output layer.

The update process is performed using the following equation,

$$O_{wi}(k+1) = \sum_{i=1}^{72} \eta.H_i^{(2)}.O_b + \delta.O_{wi}(k) \tag{14}$$

where, $O_{wi}$ is the weight value from the $i$ node in the second hidden layer to the node in the output layer, $\eta$ is the learning rate, $H_i^{(2)}$ is the value of the $i$ node in the second hidden layer, $\delta$ is the momentum factor, and $k$ is the iteration value that occurs. Then, to update the bias value in the second hidden layer, the following equation is used,

$$H_{bi}^{(2)} = \left(1 - H_i^{(2)}\right).H_i^{(2)}.P^{(2)} \tag{15}$$

where, $H_{bi}^{(2)}$ is the bias value of the $i$ node in the second hidden layer, $H_i^{(2)}$ is the value of the $i$ node in the second hidden layer, and $P^{(2)}$ is the accumulation value between the weight in the output layer ($O_{wi}$) and the bias in the output layer ($O_b$), calculated using the following equation,

$$P^{(2)} = \sum_{i=1}^{72} O_{wi}.O_b \tag{16}$$

Then, the weight values from the first hidden layer to the second hidden layer can be updated using the following equation,

$$H_{wij}^{(2)}(k+1) = \sum_{j=1}^{72}\sum_{i=1}^{120} \eta.H_i^{(1)}.H_{bj}^{(2)} + \delta.H_{wij}^{(2)}(k) \tag{17}$$

where, $H_{wij}^{(2)}$ is the weight value from the $i$ node in the first hidden layer to the $j$ node in the second hidden layer, and $H_i^{(1)}$ is the value of the $i$ node in the first hidden layer. To update the bias value in the first hidden layer, the following equation is used,

$$H_{bi}^{(1)} = \left(1 - H_i^{(1)}\right).H_i^{(1)}.P^{(1)} \tag{18}$$

where, $H_{bi}^{(1)}$ is the bias value of the $i$ node in the first hidden layer, $H_i^{(1)}$ is the value of the $i$ node in the first hidden layer, and $P^{(1)}$ is the accumulation value between the weight in the second hidden layer ($H_{wij}^{(2)}$) and the bias in the second hidden layer ($H_{bi}^{(2)}$), calculated using the following equation,

$$P^{(1)} = \sum_{j=1}^{120}\sum_{i=1}^{72} H_{wij}^{(2)}.H_{bi}^{(2)} \tag{19}$$

Then, to update the weight values from the input layer to the first hidden layer, the following equation is used,

$$H_{wij}^{(1)}(k+1) = \sum_{j=1}^{120}\sum_{i=1}^{4} \eta.I_i.H_{bj}^{(1)} + \delta.H_{wij}^{(1)}(k) \tag{20}$$

where, $H_{wij}^{(1)}$ is the weight value from the $i$ node in the input layer to the $j$ node in the first hidden layer, and $I_i$ is the value of the $i$ input node in the input layer. The learning process of this ANN continues iteratively until the specified iteration and yields small error values [68].

## IV. PERFORMANCE ANALYSIS

The analysis provides information on each model's performance results in predicting the PV power output based on its operational temperature. The analysis methods used include calculating the Mean Absolute Error (MAE), Mean Squared Error (MSE), Root Mean Squared Error (RMSE), and Coefficient of Determination ($R^2$).

MAE is one of the commonly used methods for analyzing the performance of a model. MAE measures the average of the absolute differences between the predicted values generated by the model and the actual values in the test data. This result provides an overview of how close the model's predictions are to the overall values. The equation for MAE is as follows,

$$MAE = \frac{1}{n}\sum_{i=n}^{n} \left|y_i - \hat{y}_i\right| \tag{21}$$

where, $n$ is the number of test data, $y_i$ is the actual value, and $\hat{y}_i$ is the predicted value by the model for the $i$ data. The lower the MAE value, the better the model performance, indicating that the model's predictions are closer to the actual values [69]. Furthermore, MSE is an analysis method used to measure the average of the squared differences between the predicted values generated by the model and the actual values in the test data. The equation for MSE is defined as follows,

$$MSE = \frac{1}{n}\sum_{i=n}^{n} \left(y_i - \hat{y}_i\right)^2 \tag{22}$$

If the MSE value is lower, the model's performance is better, indicating that the model's predictions are closer to the actual values. Furthermore, there is RMSE, which is similar to MSE. Still, RMSE calculates the square root of the average of the squared differences between the predicted values generated by the model and the actual values. The equation for RMSE is defined as follows,

$$RMSE = \sqrt{\frac{1}{n}\sum_{i=n}^{n} \left(y_i - \hat{y}_i\right)^2} \tag{23}$$

RMSE analysis provides insight into the average deviation between the model's predicted and actual values. By taking the square root, RMSE has a more intuitive interpretation in the same units as the target variable. Lower RMSE values indicate better model performance, indicating that the model's predictions are closer to the actual values. [70]. Then, $R^2$ analysis, also called the Coefficient of Determination, assesses how effectively the model can explain the variability observed in the data. The equation for the Coefficient of Determination is defined as follows,

$$R^2 = 1 - \frac{\sum_{i=1}^{n}(y_i - \hat{y}_i)^2}{\sum_{i=1}^{n}(y_i - \hat{y})^2} \tag{24}$$

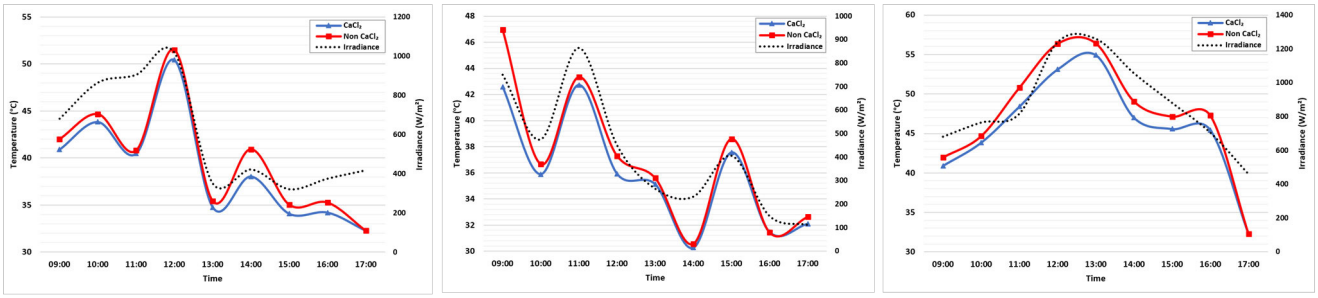


(a) (b) (c)

**FIGURE 2.** The comparison result of photovoltaic temperature on (a) day 1, (b) day 2, and (c) day 3.

where, $\hat{y}$ is the mean of all $y_i$ values, the $R^2$ value ranges from 0 to 1, and the closer it is to 1, the better the model explains the data's variability. $R^2$ analysis can determine how much of the variability in the PV output power data can be explained by the panel temperature data [71].

## V. RESULTS AND DISCUSSION

In this section, an evaluation is conducted to observe the effect of PV cooling methods using Calcium Chloride on PV temperature, power, and efficiency and to determine the performance level of the MLR, TC-P, and ANN models in predicting PV output power.

### A. PHOTOVOLTAIC POWER ANALYSIS

Figure 2 shows a graph comparing the PV temperature over time for three days, under two scenarios: when using Calcium Chloride and when not using Calcium Chloride. From the graph, it can be observed that there is a correlation between temperature and irradiance, where an increase in irradiance results in an increase in the operational temperature of the PV. This result is consistent with the initial hypothesis, considering that higher irradiance leads to more solar energy absorbed, thus raising the PV temperature. It is also noticeable that during periods of high irradiance, the PV temperature with Calcium Chloride tends to be lower than without Calcium Chloride. This demonstrates that Calcium Chloride has a significant cooling effect on the PV panel. However, in Figure 2(a), there is a strange phenomenon where irradiance increases between 10:00 and 12:00 while the temperature decreases. Several factors, such as increased wind flow, can explain this behavior. This occurs because the increased wind can carry heat away, accelerating the cooling process. Additionally, air humidity also plays a role. High humidity can enhance the cooling rate through evaporation, decreasing temperature despite increasing irradiance.

Figure 3 compares the PV power output with and without the use of Calcium Chloride. The graph shows a clear correlation between irradiance and the generated PV power. Calcium Chloride results in a more stable and higher power output than when it is not used. This indicates that Calcium Chloride may enhance electricity production by reducing its operational temperature.

**TABLE 7.** Analysis of temperature photovoltaic.

| | Avg. Irradiance ($W/m^2$) | Avg. $T_{pv}$ (°C) | | $\%T_{pv}$ Decrease |
|---|---|---|---|---|
| | | $CaCl_2$ | Non-$CaCl_2$ | |
| **Day 1** 4th April 2023 | 594.6 | 38.8 | 39.8 | 2.5% |
| **Day 2** 5th April 2023 | 412 | 36 | 37 | 2.8% |
| **Day 3** 6th April 2023 | 873.5 | 45.7 | 47.3 | 3.4% |

Figure 4 displays the PV efficiency graph over three days, comparing the use of Calcium Chloride to not using Calcium Chloride. PV efficiency is the ratio of electrical energy generated to the solar energy received. The graph shows that using Calcium Chloride can influence efficiency by maintaining the panel temperature at an optimal level. Typically, PV panels achieve higher efficiency at lower operational temperatures. The effect of using Calcium Chloride can be seen through the position of the curve, which is higher than the curve without Calcium Chloride. These results indicate the effectiveness of Calcium Chloride in managing PV temperature to enhance efficiency, considering that PV generally operates less efficiently at higher temperatures.

Table 7 depicts the analysis of PV operational temperatures measured under conditions with and without Calcium Chloride over three consecutive days in April 2023. The average PV panel temperature appears lower during the cooling process using Calcium Chloride. In contrast, in the absence of Calcium Chloride, the average PV panel temperature consistently appears higher, by around 1°C, than that of panels using Calcium Chloride. Based on these results, Calcium Chloride effectively reduces operational temperatures, enhancing PV systems efficiency. Table 8 shows the analysis of the effect of power generated by PV systems under conditions with and without Calcium Chloride. During the cooling process with Calcium Chloride, there was an increase in power output from the PV systems. The highest percentage increase in power, reaching 11.7%,

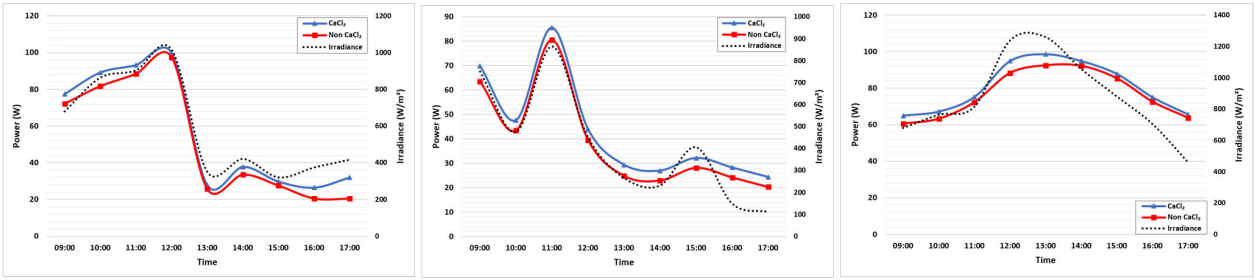


**FIGURE 3.** The comparison result of photovoltaic power on (a) day 1, (b) day 2, and (b) day 3.

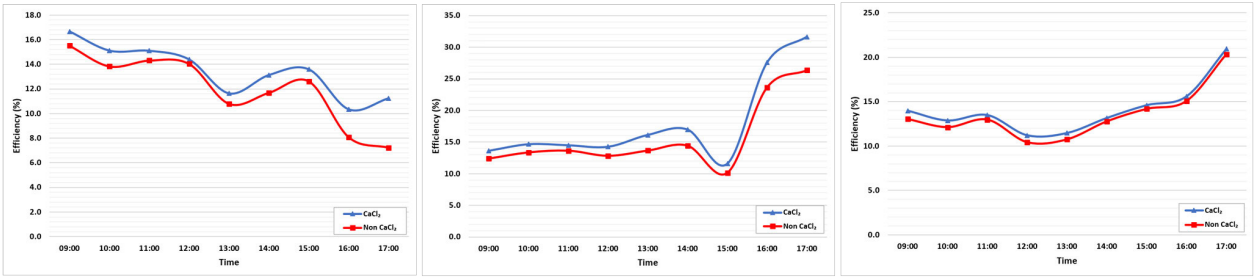


**FIGURE 4.** The comparison result of photovoltaic efficiency on (a) day 1, (b) day 2, and (b) day 3.

**TABLE 8.** Analysis of power photovoltaic.

| | Avg. Irradiance ($W/m^2$) | Total $P_{pv}$ (W) | | $\%P_{pv}$ Increase |
|---|---|---|---|---|
| | | $CaCl_2$ | Non-$CaCl_2$ | |
| **Day 1** 4th April 2023 | 594.6 | 514 | 468.1 | 9.8% |
| **Day 2** 5th April 2023 | 412 | 387.9 | 347.3 | 11.7% |
| **Day 3** 6th April 2023 | 873.5 | 724.9 | 691.1 | 4.9% |

**TABLE 9.** The comparative evaluation with other cooling methods.

| Cooling Method | Maximum Irradiance ($W/m^2$) | Efficiency Improvement (%) |
|---|---|---|
| CNT/$Al_2O_3$ Hybrid [54] | 677.41 | 2.4 |
| Aluminum Heatsink [55] | 1000 | 2.6 |
| $Al_2O_3$/PCM Mixture [56] | 650.8 | 10.9 |
| $TiO_2$ [57] | 750 | 0.82 |
| Zn/$H_2O$ Mixture [59] | 900 | 7.8 |
| Water [61] | - | 12.5 |
| $CaCl_2$ (Proposed Method) | 873.5 | 11.3 |

indicates higher effectiveness of Calcium Chloride under low irradiance conditions. Conversely, the lowest increase in power, at 4.9%, suggests that under higher irradiance conditions, the effectiveness of Calcium Chloride is not as pronounced as under low irradiance conditions. Based on these findings, it can be concluded that using Calcium Chloride impacts electrical power production in PV systems. The magnitude of this power increase varies depending on daily irradiance conditions. Table 9 compares the proposed PV cooling method with previously evaluated cooling technologies. Based on this comparison, it can be concluded that the proposed Calcium Chloride cooling method demonstrates an average efficiency improvement of 11.3%, which is almost comparable to the cooling method using water. This evaluation indicates that the effectiveness of various cooling methods depends on the type of cooling material and the irradiance conditions.

### B. MODELS PERFORMANCE ANALYSIS

Figure 5 shows the correlation between PV power measurement data and prediction data using the MLR model. The graph displays clustered data around the regression line, indicating a strong correlation between the predicted and actual data. Although some points deviate from the line, the MLR model makes relatively accurate predictions. The data spread is wider at the bottom of the graph than at the top, indicating more significant prediction variability.

Figure 6 illustrates the correlation between the predicted and measured PV power data using the TC-P model. In the graph, the gradient of the line is almost close to 1, indicating that for every increase in power predicted by the TC-P model, the measured PV power also increases almost proportionally. This can be interpreted as the model having nearly perfect predictive proportionality to the measured values. Only a few data points are far from the line, indicating consistent and accurate predictions in many cases. Figure 7 shows the correlation graph between the predicted PV power data using the ANN model and the actual power. In the graph,

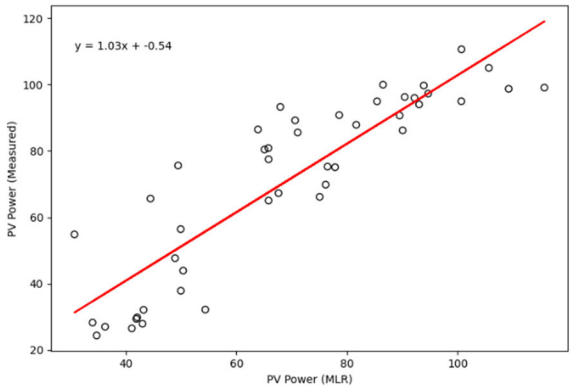


**FIGURE 5.** The correlation between prediction data and measured photovoltaic power using the MLR model.

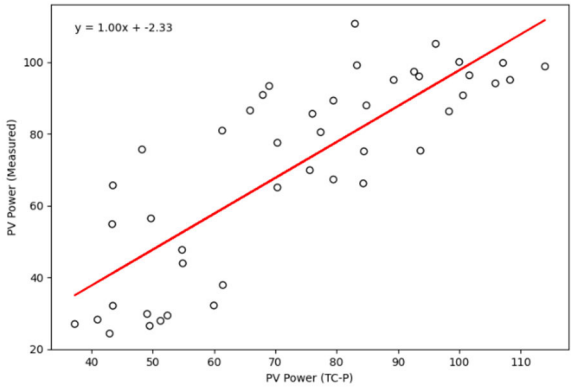


**FIGURE 6.** The correlation between prediction data and measured photovoltaic power using the TC-P model.

the gradient of the line is slightly greater than 1, indicating that the model's predictions are somewhat higher than the actual measurement values for each data point. The density of data points near the regression line suggests that the ANN model strongly correlates with the measured values. The regression line almost blending with the data points indicates a very high level of conformity between the model's predictions and the actual data. This consistency demonstrates the success of training the ANN model in mapping the relationship between the input variables and the PV power output. However, some data points far from the regression line indicate errors in specific predictions.

From the analysis results, a comparison of the model performance is presented in Table 10. The ANN model outperforms the other two models by a significant margin based on the data. This is apparent from the $R^2$ value, which approaches 1, indicating a very high level of variability explained by the model. Additionally, the ANN model's MAE, MSE, and RMSE values are much lower than the other two, indicating more minor prediction errors. Therefore, the ANN model is better for accurately predicting power output based on the given thermal condition data.

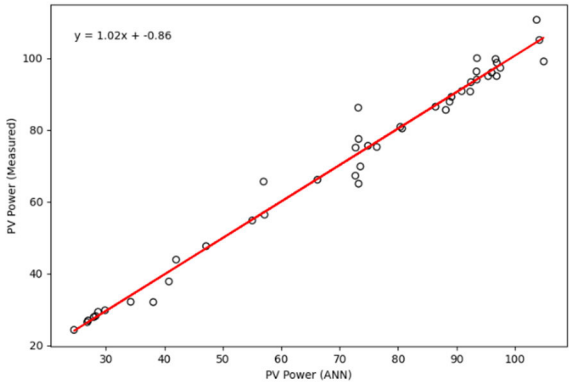


**FIGURE 7.** The correlation between prediction data and measured photovoltaic power using the ANN model.

**TABLE 10.** The comparison of models' performance.

| Model | $R^2$ | MAE | MSE | RMSE |
|---|---|---|---|---|
| MLR | 0.78 | 10.3 | 157.2 | 12.5 |
| TC-P | 0.67 | 13.5 | 240.7 | 15.5 |
| ANN | 0.98 | 2.3 | 13.3 | 3.6 |

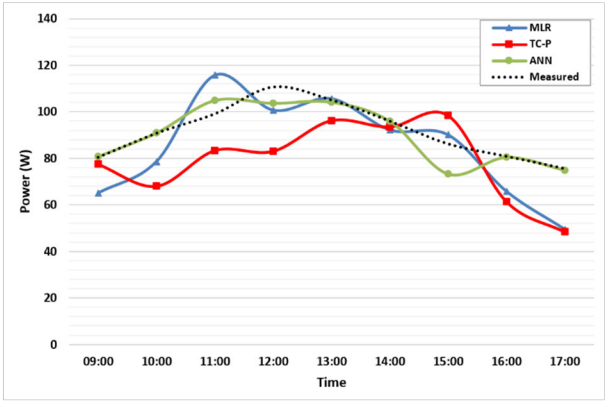


**FIGURE 8.** The comparison result of prediction power ($E = 970\,W/m^2$, $T_{pv} = 43.6°C$).

### C. POWER PREDICTION ANALYSIS

Figure 8 shows the comparison results of power predictions from various models against actual measurements on the PV panel, under irradiance conditions of 970 W/m$^2$ and a PV panel temperature of 43.6°C. All prediction models exhibit a similar pattern to the actual measurement data, with fluctuations in power occurring over time. The ANN model curve provides predictions that closely match the actual measurements, following the trend well and with the slightest variation. Conversely, the MLR model curve shows more variable predictions, with some peaks and troughs not aligning with the actual data. Then, the TC-P model curve exhibits significant variations from the actual data, especially around midday, where its predictions are much higher than the actual measurements.

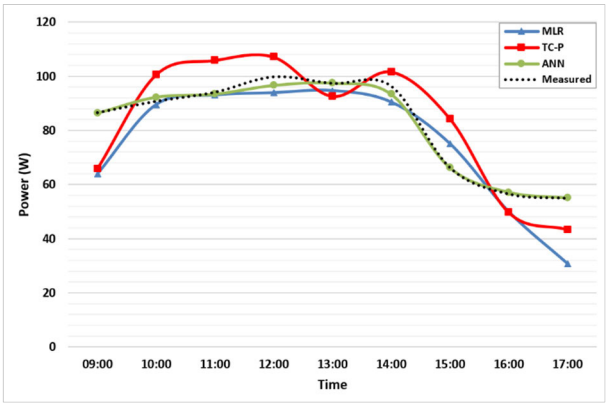


**FIGURE 9.** The comparison result of prediction power ($E = 840\,W/m^2$, $T_{pv} = 45.1°C$).

Figure 9 compares power predictions generated by several models against actual measurements, with irradiance conditions of 840 W/m$^2$ and the PV panel temperature of 45.1°C. Like the previous graph, all models exhibit a similar trend to the actual measurements. The ANN model curve provides results very close to the exact measurements, with reasonable adjustments to the power fluctuations throughout the day. On the other hand, the TC-P model curve also approximates the measurements but shows slight deviations, especially towards midday. Then, the MLR model curve has more noticeable deviations from the actual data than the other two models, particularly around midday, where its predictions are lower than the exact measurements.

Based on these results, it can be concluded that the ANN and TC-P models exhibit more accurate results than MLR in this condition, with ANN being the best among the three models. This indicates that the ANN model performs better in high data variability and non-linear conditions.

## VI. CONCLUSION

This study demonstrates that using Calcium Chloride ($CaCl_2$) as a coolant on PV panels effectively reduces the operating temperature by up to 4.4°C, with an average temperature decrease of 2.9% compared to conditions without Calcium Chloride. This cooling method can also increase PV power by up to 55.8W, with an average power increase of 8.8%, compared to not using Calcium Chloride. PV efficiency also experiences a 5.3% increase compared to conditions without Calcium Chloride. Furthermore, modeling was conducted using MLR, TC-P, and ANN to predict PV output power based on variations in operating temperature using Calcium Chloride as a coolant. The results show that the ANN model performs better in predicting PV output power. This confirms that the ANN model can understand the complexity of the relationship between operating temperature and PV power. These findings provide insights into the benefits of using Calcium Chloride compounds as cooling materials on PV panels and the potential of ANN as an effective predictive model. Based on the exergy aspect, the system with Calcium Chloride cooling has higher exergy than without because the lower PV temperature can increase electrical energy conversion efficiency and reduce energy losses.

While using Calcium Chloride in cooling offers several significant advantages, some limitations must be considered. Firstly, this study is limited to testing conducted at more than one specific location, which may not represent the environmental variations at other places. Secondly, the long-term impacts of using Calcium Chloride in PV systems still need to be fully understood. Therefore, further research is required to test the effectiveness of the coolant Calcium Chloride method on a larger scale and under various environmental conditions, including broader geographical and climatic variations. Additionally, studies on the potential corrosive effects or other impacts that may arise from using Calcium Chloride compounds on PV and a Life Cycle Assessment (LCA) are necessary to understand the long-term environmental effects of using Calcium Chloride.

## REFERENCES

[1] G. Todorov, H. Vasilev, K. Kamberov, T. Ivanov, and Y. Sofronov, "Concept and virtual prototyping of cooling module for photovoltaic system," in *Proc. 6th Int. Symp. Environ.-Friendly Energies Appl. (EFEA)*, Mar. 2021, pp. 1–4, doi: 10.1109/EFEA49713.2021.9406247.

[2] A. K. Tripathi, S. Ray, and M. Aruna, "Analysis on photovoltaic panel temperature under the influence of solar radiation and ambient temperature," in *Proc. Int. Conf. Adv. Electr., Comput., Commun. Sustain. Technol. (ICAECT)*, Feb. 2021, pp. 1–5, doi: 10.1109/ICAECT49130.2021.9392619.

[3] A. Risdiyanto, Ant. A. Kristi, B. Susanto, N. A. Rachman, A. Junaedi, and E. W. Mukti, "Implementation of photovoltaic water spray cooling system and its feasibility analysis," in *Proc. Int. Conf. Sustain. Energy Eng. Appl. (ICSEEA)*, Nov. 2020, pp. 88–93, doi: 10.1109/ICSEEA50711.2020.9306133.

[4] E. Skoplaki and J. A. Palyvos, "On the temperature dependence of photovoltaic module electrical performance: A review of efficiency/power correlations," *Sol. Energy*, vol. 83, no. 5, pp. 614–624, May 2009, doi: 10.1016/j.solener.2008.10.008.

[5] J. Oh, B. Rammohan, A. Pavgi, S. Tatapudi, G. Tamizhmani, G. Kelly, and M. Bolen, "Reducing photovoltaic module temperature using improved backsheet materials," in *Proc. IEEE 7th World Conf. Photovoltaic Energy Convers. (WCPEC) (Joint Conf. 45th IEEE PVSC, 28th PVSEC 34th EU PVSEC)*, Jun. 2018, pp. 2826–2831, doi: 10.1109/PVSC.2018.8547275.

[6] T. Wongwuttanasatian, T. Sarikarin, and A. Suksri, "Performance enhancement of a photovoltaic module by passive cooling using phase change material in a finned container heat sink," *Sol. Energy*, vol. 195, pp. 47–53, Jan. 2020, doi: 10.1016/j.solener.2019.11.053.

[7] D. C. Jordan, K. Perry, R. White, and C. Deline, "Extreme weather and PV performance," *IEEE J. Photovolt.*, vol. 13, no. 6, pp. 830–835, Nov. 2023, doi: 10.1109/JPHOTOV.2023.3304357.

[8] O. Dupré, R. Vaillon, and M. A. Green, *Thermal Behavior of Photovoltaic Devices*. Cham, Switzerland: Springer, 2017.

[9] S. Chandra, A. Yadav, M. A. R. Khan, M. Pushkarna, M. Bajaj, and N. K. Sharma, "Influence of artificial and natural cooling on performance parameters of a solar PV system: A case study," *IEEE Access*, vol. 9, pp. 29449–29457, 2021, doi: 10.1109/ACCESS.2021.3058779.

[10] H. G. Teo, P. S. Lee, and M. N. A. Hawlader, "An active cooling system for photovoltaic modules," *Appl. Energy*, vol. 90, no. 1, pp. 309–315, Feb. 2012, doi: 10.1016/j.apenergy.2011.01.017.

[11] P. K. Dash and N. C. Gupta, "Effect of temperature on power output from different commercially available photovoltaic modules," *J. Eng. Res. Appl.*, vol. 5, no. 1, pp. 1–4, 2015. [Online]. Available: www.ijera.com

[12] M. Seapan, Y. Hishikawa, M. Yoshita, and K. Okajima, "Temperature and irradiance dependences of the current and voltage at maximum power of crystalline silicon PV devices," *Sol. Energy*, vol. 204, pp. 459–465, Jul. 2020, doi: 10.1016/j.solener.2020.05.019.

[13] T. Yu, C. Ren, Y. Jia, J. Li, J. Zhang, Y. Xu, B. Yan, M. Zhang, L. Qiao, T. Wang, and S. Gao, "Photovoltaic panel temperature monitoring and prediction by Raman distributed temperature sensor with fuzzy temperature difference threshold method," *IEEE Sensors J.*, vol. 21, no. 1, pp. 373–380, Jan. 2021, doi: 10.1109/JSEN.2020.3015508.

[14] A. Gok, E. Ozkalay, G. Friesen, and F. Frontini, "The influence of operating temperature on the performance of BIPV modules," *IEEE J. Photovolt.*, vol. 10, no. 5, pp. 1371–1378, Sep. 2020, doi: 10.1109/JPHOTOV.2020.3001181.

[15] S. Nižetić, D. Čoko, A. Yadav, and F. Grubišić-Čabo, "Water spray cooling technique applied on a photovoltaic panel: The performance response," *Energy Convers. Manage.*, vol. 108, pp. 287–296, Jan. 2016, doi: 10.1016/j.enconman.2015.10.079.

[16] K. Rishi, M. Balachandran, G. Raagul, A. Srinivasagopalan, B. Ramkiran, and P. Neelamegam, "Solar cooling technologies–A review," in *Proc. Int. Conf. Comput. Power, Energy, Inf. Commun. (ICCPEIC)*, Mar. 2018, pp. 174–178, doi: 10.1109/ICCPEIC.2018.8525162.

[17] S. Kalaiselvan, V. Karthikeyan, G. Rajesh, A. S. Kumaran, B. Ramkiran, and P. Neelamegam, "Solar PV active and passive cooling technologies—A review," in *Proc. Int. Conf. Comput. Power, Energy, Inf. Commun. (ICCPEIC)*, Mar. 2018, pp. 166–169, doi: 10.1109/ICCPEIC.2018.8525185.

[18] F. Rahmaniah, W. Zhang, and S. E. R. Tay, "State space transient model for photovoltaic module temperature estimation," in *Proc. 47th IEEE Photovoltaic Spec. Conf. (PVSC)*, Jun. 2020, pp. 2505–2508, doi: 10.1109/pvsc45281.2020.9300581.

[19] H. Najafi and K. A. Woodbury, "Optimization of a cooling system based on Peltier effect for photovoltaic cells," *Sol. Energy*, vol. 91, pp. 152–160, May 2013, doi: 10.1016/j.solener.2013.01.026.

[20] S. Dubey, J. N. Sarvaiya, and B. Seshadri, "Temperature dependent photovoltaic (PV) efficiency and its effect on PV production in the world—A review," *Energy Proc.*, vol. 33, pp. 311–321, Jan. 2013, doi: 10.1016/j.egypro.2013.05.072.

[21] W. G. Anderson, P. M. Dussinger, D. B. Sarraf, and S. Tamanna, "Heat pipe cooling of concentrating photovoltaic cells," in *Proc. 33rd IEEE Photovolatic Spec. Conf.*, May 2008, pp. 1–6, doi: 10.1109/PVSC.2008.4922577.

[22] T. J. Silverman, M. G. Deceglie, I. Subedi, N. J. Podraza, I. M. Slauch, V. E. Ferry, and I. Repins, "Reducing operating temperature in photovoltaic modules," *IEEE J. Photovolt.*, vol. 8, no. 2, pp. 532–540, Mar. 2018, doi: 10.1109/JPHOTOV.2017.2779842.

[23] P. K. Pathak, D. G. Roy, A. K. Yadav, S. Padmanaban, F. Blaabjerg, and B. Khan, "A state-of-the-art review on heat extraction methodologies of photovoltaic/thermal system," *IEEE Access*, vol. 11, pp. 49738–49759, 2023, doi: 10.1109/ACCESS.2023.3277728.

[24] M. Libra, T. Petrík, V. Poulek, I. I. Tyukhov, and P. Kourím, "Changes in the efficiency of photovoltaic energy conversion in temperature range with extreme limits," *IEEE J. Photovolt.*, vol. 11, no. 6, pp. 1479–1484, Nov. 2021, doi: 10.1109/JPHOTOV.2021.3108484.

[25] T. Özden, D. Tolgay, and B. G. Akinoglu, "Daily and monthly module temperature variation for 9 different modules," in *Proc. Int. Conf. Photovoltaic Sci. Technol. (PVCon)*, Jul. 2018, pp. 4849–4854, doi: 10.1109/PVCon.2018.8523878.

[26] D. T. Cotfas, P. A. Cotfas, and O. M. Machidon, "Study of temperature coefficients for parameters of photovoltaic cells," *Int. J. Photoenergy*, vol. 2018, pp. 1–12, Jan. 2018, doi: 10.1155/2018/5945602.

[27] Y. Away and I. D. Sara, "The effect of adding a heatsink as a coolant to increasing output power at solar panels," in *Proc. 7th Int. Conf. Electr., Telecommun. Comput. Eng. (ELTICOM)*, Dec. 2023, pp. 111–115, doi: 10.1109/elticom61905.2023.10443116.

[28] H. A. Kazem, A. A. Al-Waeli, M. T. Chaichan, K. Sopian, A.-A. Ahmed, and W. I. W. N. Roslam, "Enhancement of photovoltaic module performance using passive cooling (Fins): A comprehensive review," *Case Stud. Thermal Eng.*, vol. 49, Sep. 2023, Art. no. 103316, doi: 10.1016/j.csite.2023.103316.

[29] M. Bouché, M. Richter, and M. Linder, "Heat transformation based on $CaCl_2/H_2O$—Part B: Open operation principle," *Appl. Thermal Eng.*, vol. 102, pp. 641–647, Jun. 2016, doi: 10.1016/j.applthermaleng.2016.03.102.

[30] M. Tokarev, L. Gordeeva, V. Romannikov, I. Glaznev, and Y. Aristov, "New composite sorbent $CaCl_2$ in mesopores for sorption cooling/heating," *Int. J. Thermal Sci.*, vol. 41, no. 5, pp. 470–474, Apr. 2002, doi: 10.1016/s1290-0729(02)01339-x.

[31] Y. Li, X. Xu, X. Wang, P. Li, Q. Hao, and B. Xiao, "Survey and evaluation of equations for thermophysical properties of binary/ternary eutectic salts from NaCl, KCl, $MgCl_2$, $CaCl_2$, $ZnCl_2$ for heat transfer and thermal storage fluids in CSP," *Sol. Energy*, vol. 152, pp. 57–79, Aug. 2017, doi: 10.1016/j.solener.2017.03.019.

[32] F. Bayrak, H. F. Oztop, and F. Selimefendigil, "Experimental study for the application of different cooling techniques in photovoltaic (PV) panels," *Energy Convers. Manage.*, vol. 212, May 2020, Art. no. 112789, doi: 10.1016/j.enconman.2020.112789.

[33] M. Richter, M. Bouché, and M. Linder, "Heat transformation based on $CaCl_2/H_2O$—Part A: Closed operation principle," *Appl. Thermal Eng.*, vol. 102, pp. 615–621, Jun. 2016, doi: 10.1016/j.applthermaleng.2016.03.076.

[34] D. Wei, Q. Cui, E. Gao, P. Qi, and X. Zhang, "Study on the heat transfer characteristics of $CO_2$ and liquid desiccant $CaCl_2$ aqueous solution in the gas cooler and evaporator," *Int. J. Thermal Sci.*, vol. 197, Mar. 2024, Art. no. 108830, doi: 10.1016/j.ijthermalsci.2023.108830.

[35] K. C. Chan, C. Y. H. Chao, and M. Bahrami, "Heat and mass transfer characteristics of a zeolite $13X/CaCl_2$ composite adsorbent in adsorption cooling systems," in *Proc. ASME 6th Int. Conf. Energy Sustainability, Parts A B*, Jul. 2012, pp. 49–58, doi: 10.1115/es2012-91246.

[36] T. Ibrahim, M. A. Akrouch, F. Hachem, M. Ramadan, H. S. Ramadan, and M. Khaled, "Cooling techniques for enhanced efficiency of photovoltaic panels—Comparative analysis with environmental and economic insights," *Energies*, vol. 17, no. 3, p. 713, Feb. 2024, doi: 10.3390/en17030713.

[37] B. Ray, R. Shah, M. R. Islam, and S. Islam, "A new data driven long-term solar yield analysis model of photovoltaic power plants," *IEEE Access*, vol. 8, pp. 136223–136233, 2020, doi: 10.1109/ACCESS.2020.3011982.

[38] X. Cheng, J. Wu, D.-X. Li, and X. Zhu, "The method for photovoltaic module temperature short-term forecasting based on numerical weather prediction," in *Proc. 3rd Asia Energy Electr. Eng. Symp. (AEEES)*, Mar. 2021, pp. 938–941, doi: 10.1109/AEEES51875.2021.9403159.

[39] A. Driesse, M. Theristis, and J. S. Stein, "A new photovoltaic module efficiency model for energy prediction and rating," *IEEE J. Photovolt.*, vol. 11, no. 2, pp. 527–534, Mar. 2021, doi: 10.1109/JPHOTOV.2020.3045677.

[40] P. Ramsami and V. Oree, "A hybrid method for forecasting the energy output of photovoltaic systems," *Energy Convers. Manage.*, vol. 95, pp. 406–413, May 2015, doi: 10.1016/j.enconman.2015.02.052.

[41] G. G. Kim, J. H. Choi, S. Y. Park, B. G. Bhang, W. J. Nam, H. L. Cha, N. Park, and H.-K. Ahn, "Prediction model for PV performance with correlation analysis of environmental variables," *IEEE J. Photovolt.*, vol. 9, no. 3, pp. 832–841, May 2019, doi: 10.1109/JPHOTOV.2019.2898521.

[42] G. Moreno, P. Martin, C. Santos, F. J. Rodríguez, and E. Santiso, "A day-ahead irradiance forecasting strategy for the integration of photovoltaic systems in virtual power plants," *IEEE Access*, vol. 8, pp. 204226–204240, 2020, doi: 10.1109/ACCESS.2020.3036140.

[43] G. Makrides, B. Zinsser, A. Phinikarides, M. Schubert, and G. E. Georghiou, "Temperature and thermal annealing effects on different photovoltaic technologies," *Renew. Energy*, vol. 43, pp. 407–417, Jul. 2012, doi: 10.1016/j.renene.2011.11.046.

[44] E. C. Asiri, C. Y. Chung, and X. Liang, "Day-ahead prediction of distributed regional-scale photovoltaic power," *IEEE Access*, vol. 11, pp. 27303–27316, 2023, doi: 10.1109/ACCESS.2023.3258449.
[45] A. Zielinska, M. Skowron, and A. Bien, "Modelling of photovoltaic cells in variable conditions of temperature and intensity of solar insolation as a method of mapping the operation of the installation in real conditions," in *Proc. Int. Interdiscipl. PhD Workshop (IIPhDW)*, May 2018, pp. 200–204, doi: 10.1109/IIPHDW.2018.8388357.
[46] M. Prilliman, J. S. Stein, D. Riley, and G. Tamizhmani, "Transient weighted moving average model of photovoltaic module back-surface temperature," *IEEE J. Photovolt.*, vol. 10, no. 4, pp. 490–497, May 2020, doi: 10.1109/PVSC45281.2020.9300872.
[47] A. K. Yadav and S. S. Chandel, "Identification of relevant input variables for prediction of 1-minute time-step photovoltaic module power using artificial neural network and multiple linear regression models," *Renew. Sustain. Energy Rev.*, vol. 77, pp. 955–969, Sep. 2017, doi: 10.1016/j.rser.2016.12.029.
[48] M. Ayan and H. Toylan, "Estimating the power generating of a stand-alone solar photovoltaic panel using artificial neural networks and statistical methods.," *Energy Sources, A, Recovery, Utilization, Environ. Effects*, vol. 43, no. 20, pp. 2496–2508, Nov. 2020, doi: 10.1080/15567036.2020.1849459.
[49] R. Dubey, P. Batra, S. Chattopadhyay, A. Kottantharayil, B. M. Arora, K. L. Narasimhan, and J. Vasi, "Measurement of temperature coefficient of photovoltaic modules in field and comparison with laboratory measurements," in *Proc. IEEE 42nd Photovoltaic Spec. Conf. (PVSC)*, Jun. 2015, pp. 1–5, doi: 10.1109/PVSC.2015.7355852.
[50] S. Al-Dahidi, M. Louzazni, and N. Omran, "A local training strategy-based artificial neural network for predicting the power production of solar photovoltaic systems," *IEEE Access*, vol. 8, pp. 150262–150281, 2020, doi: 10.1109/ACCESS.2020.3016165.
[51] M. A. Khan, M. A. Khan, H. Ali, B. Ashraf, S. Khan, D.-E.-Z. Baig, A. Wadood, and T. Khurshaid, "Output power prediction of a photovoltaic module through artificial neural network," *IEEE Access*, vol. 10, pp. 116160–116166, 2022, doi: 10.1109/ACCESS.2022.3216384.
[52] S. Al-Dahidi, O. Ayadi, M. Alrbai, and J. Adeeb, "Ensemble approach of optimized artificial neural networks for solar photovoltaic power prediction," *IEEE Access*, vol. 7, pp. 81741–81758, 2019, doi: 10.1109/ACCESS.2019.2923905.
[53] S. Samara and E. Natsheh, "Intelligent real-time photovoltaic panel monitoring system using artificial neural networks," *IEEE Access*, vol. 7, pp. 50287–50299, 2019, doi: 10.1109/ACCESS.2019.2911250.
[54] R. Sathyamurthy, A. E. Kabeel, A. Chamkha, A. Karthick, A. M. Manokar, and M. G. Sumithra, "Experimental investigation on cooling the photovoltaic panel using hybrid nanofluids," *Appl. Nanosci.*, vol. 11, no. 2, pp. 363–374, Feb. 2021, doi: 10.1007/s13204-020-01598-2.
[55] Z. Arifin, D. D. D. P. Tjahjana, S. Hadi, R. A. Rachmanto, G. Setyohandoko, and B. Sutanto, "Numerical and experimental investigation of air cooling for photovoltaic panels using aluminum heat sinks," *Int. J. Photoenergy*, vol. 2020, pp. 1–9, Jan. 2020, doi: 10.1155/2020/1574274.
[56] M. R. Salem, M. M. Elsayed, A. A. Abd-Elaziz, and K. M. Elshazly, "Performance enhancement of the photovoltaic cells using $Al_2O_3$/PCM mixture and/or water cooling-techniques," *Renew. Energy*, vol. 138, pp. 876–890, Aug. 2019, doi: 10.1016/j.renene.2019.02.032.
[57] M. S. Y. Ebaid, A. M. Ghrair, and M. Al-Busoul, "Experimental investigation of cooling photovoltaic (PV) panels using ($TiO_2$) nanofluid in water-polyethylene glycol mixture and ($Al_2O_3$) nanofluid in water-cetyltrimethylammonium bromide mixture," *Energy Convers. Manage.*, vol. 155, pp. 324–343, Jan. 2018, doi: 10.1016/j.enconman.2017.10.074.
[58] P. Mundle, S. Chattopadhyay, C. S. Solanki, N. Shiradkar, A. Kottantharayil, K. L. Narasimhan, J. Vasi, and B. K. Chakravarthy, "Effect of aluminum back plate on PV module temperature and performance," in *Proc. IEEE 7th World Conf. Photovoltaic Energy Convers. (WCPEC) (Joint Conf. 45th IEEE PVSC, 28th PVSEC 34th EU PVSEC)*, Jun. 2018, pp. 745–748, doi: 10.1109/PVSC.2018.8547921.
[59] H. A. Hussein, A. H. Numan, and R. A. Abdulrahman, "Improving the hybrid photovoltaic/thermal system performance using water-cooling technique and Zn-$H_2O$ nanofluid," *Int. J. Photoenergy*, vol. 2017, no. 3, pp. 1–14, 2017, doi: 10.1155/2017/6919054.
[60] A. R. Amelia, Y. M. Irwan, M. Irwanto, W. Z. Leow, N. Gomesh, I. Safwati, and M. A. M. Anuar, "Cooling on photovoltaic panel using forced air convection induced by DC fan," *Int. J. Electr. Comput. Eng. (IJECE)*, vol. 6, no. 2, p. 526, Apr. 2016, doi: 10.11591/ijece.v6i2.9118.
[61] K. A. Moharram, M. S. Abd-Elhady, H. A. Kandil, and H. El-Sherif, "Enhancing the performance of photovoltaic panels by water cooling," *Ain Shams Eng. J.*, vol. 4, no. 4, pp. 869–877, Dec. 2013, doi: 10.1016/j.asej.2013.03.005.
[62] M. Kayri, I. Kayri, and M. T. Gencoglu, "The performance comparison of multiple linear regression, random forest and artificial neural network by using photovoltaic and atmospheric data," in *Proc. 14th Int. Conf. Eng. Modern Electr. Syst. (EMES)*, Jun. 2017, pp. 1–4, doi: 10.1109/EMES.2017.7980368.
[63] A. Virtuani, D. Pavanello, and G. Friesen, "Overview of temperature coefficients of different thin film photovoltaic technologies," in *Proc. 25th Eur. Photovoltaic Solar Energy Conf. Exhib./5th World Conf. Photovoltaic Energy Convers.*, 2010, pp. 4248–4252, doi: 10.4229/25thEUPVSEC2010-4AV.3.83.
[64] P. Kamkird, N. Ketjoy, W. Rakwichian, and S. Sukchai, "Investigation on temperature coefficients of three types photovoltaic module technologies under Thailand operating condition," *Proc. Eng.*, vol. 32, pp. 376–383, Jan. 2012, doi: 10.1016/j.proeng.2012.01.1282.
[65] Y. Hishikawa, T. Doi, M. Higa, K. Yamagoe, H. Ohshima, T. Takenouchi, and M. Yoshita, "Voltage-dependent temperature coefficient of the I–V curves of crystalline silicon photovoltaic modules," *IEEE J. Photovolt.*, vol. 8, no. 1, pp. 48–53, Jan. 2018, doi: 10.1109/JPHOTOV.2017.2766529.
[66] C. Renno, F. Petito, and A. Gatto, "ANN model for predicting the direct normal irradiance and the global radiation for a solar application to a residential building," *J. Cleaner Prod.*, vol. 135, pp. 1298–1316, Nov. 2016, doi: 10.1016/j.jclepro.2016.07.049.
[67] G. Dosymbetova, S. Mekhilef, S. Orynbassar, A. Kapparova, A. Saymbetov, M. Nurgaliyev, B. Zholamanov, N. Kuttybay, S. Manakov, Y. Svanbayev, and N. Koshkarbay, "Neural network based active cooling system with IoT monitoring and control for LCPV silicon solar cells," *IEEE Access*, vol. 11, pp. 52585–52602, 2023, doi: 10.1109/ACCESS.2023.3280265.
[68] M. Yilmaz, R. Celikel, and A. Gundogdu, "Enhanced photovoltaic systems performance: Anti-windup PI controller in ANN-based ARV MPPT method," *IEEE Access*, vol. 11, pp. 90498–90509, 2023, doi: 10.1109/ACCESS.2023.3290316.
[69] W. Wang and Y. Lu, "Analysis of the mean absolute error (MAE) and the root mean square error (RMSE) in assessing rounding model," *IOP Conf. Ser. Mater. Sci. Eng.*, vol. 324, no. 1, 2018, Art. no. 012049, doi: 10.1088/1757-899X/324/1/012049.
[70] T. Chai and R. R. Draxler, "Root mean square error (RMSE) or mean absolute error (MAE)—Arguments against avoiding RMSE in the literature," *Geosci. Model Develop.*, vol. 7, no. 3, pp. 1247–1250, Jun. 2014, doi: 10.5194/gmd-7-1247-2014.
[71] A. Bai, J. Popp, P. Balogh, Z. Gabnai, B. Pályi, I. Farkas, G. Pintér, and H. Zsiborács, "Technical and economic effects of cooling of monocrystalline photovoltaic modules under Hungarian conditions," *Renew. Sustain. Energy Rev.*, vol. 60, pp. 1086–1099, Jul. 2016, doi: 10.1016/j.rser.2016.02.003.

**ASRI** (Student Member, IEEE) received the Graduate degree from the Faculty of Technology, Department of Electrical Engineering, Malikussaleh University, in 1991, and the master's degree from the Faculty of Engineering, Department of Electrical and System Engineering, in 2004, in coursework and research mode of study with Gajah Mada University. He is currently a Permanent Lecturer with the Department of Electrical Engineering, Universitas Malikussaleh. Teaching courses in electric power distribution, renewable energy, control, and protection systems.

**YUWALDI AWAY** (Member, IEEE) was born in South Aceh, Indonesia, in 1964. He received the degree in electrical-computer engineering from the Sepuluh Nopember Institute of Technology (ITS), Indonesia, in 1988, the M.Sc. degree from Bandung Institute of Technology (ITB), Indonesia, in 1993, and the Ph.D. degree in industrial computer from the National University of Malaysia (UKM), in 2000. Since 1990, he has been a Lecturer with the Department of Electrical and Computer Engineering, Syiah Kuala University, Indonesia, from 1996 to 2000. He was a Research Assistant and a Lecturer with the National University of Malaysia, in 2001 and 2004. Since 2007, he has been a Professor and the Head of the Research Group for Automation and Robotics Studies, Syiah Kuala University. His research interests include theory and practical, including microprocessor-based systems, simulation, automation, and optimization.

**NASARUDDIN** (Member, IEEE) received the Engineering degree in physical electronics and informatics from the Graduate School of Engineering, and the master's and Doctorate degrees from Osaka City University, Japan, in 2009. Currently, he is the Head of the Laboratory with the Department of Electrical and Computer Engineering, Syiah Kuala University. His research interests include digital communications, information theory, wireless communications, optical communications, and ICT applications for disaster.

**IRA DEVI SARA** (Member, IEEE) received the master's degree in electrical engineering from Monash University. She was involved in the polychromatic determination of the spectral response of photovoltaic devices. Her master's project was the feasibility of integrating wind power systems with hydrogen storage for victorian coastal sites. She is currently the Head of the Power Electronic and Renewable Energy Laboratory, Department of Electrical and Computer Engineering, Syiah Kuala University. Her research interests include the applied photovoltaic systems, power electronics, and renewable energies.

**ANDRI NOVANDRI** (Student Member, IEEE) was born in Aek Kanopan, North Sumatra, in 1994. He received the Bachelor of Engineering degree in electrical and computer engineering from Syiah Kuala University (USK), in 2017, and the Master of Engineering degree, in 2023. Since 2018, he has been a Research Assistant with Syiah Kuala University. After completing the master's studies, in 2023, he began teaching as a Lecturer with Ar-Raniry State Islamic University (UINAR) and Bina Bangsa Getsempena University (UBBG). His research interests include embedded systems, robotics, automation and control systems, sensors, and neural networks.